Appeared in International Conference on Noise and Vibration Engineering, Leuven, Belgium, September 13-15, 2000.

Time Series Analyses for Locating Damage Sources in Vibration Systems

Hoon Sohn[1] and Charles R. Farrar[2]
Engineering Analysis Group (ESA-EA), M/S P946
Los Alamos National Laboratory, Los Alamos, New Mexico 87545, U.S.A.

Abstract

A novel time series analysis procedure is presented to localize damage sources in a mechanical system. An attempt is made to pinpoint the sources of nonlinear damage by solely analysing the vibration signatures recorded from a structure of interests. First, a linear prediction model, combining Auto-Regressive (AR) and Auto-Regressive with eXogenous inputs (ARX) techniques, is estimated using a time series recorded under an undamaged stage of the structure. Then, the residual error, which is the difference between the actual time measurement and the prediction from the previously estimated AR-ARX combined model, is defined as our damage-sensitive feature. This study is based on the premise that if there were damage in the structure, the prediction model previously identified using the undamaged time history data would not be able to reproduce the newly obtained time series data measured under a damaged state of the structure. Furthermore, the increase of the residual errors would be maximised at the sensors instrumented near the actual damage locations. The applicability of this approach is demonstrated using the vibration test data obtained from an eight degrees-of-freedom (DOF) mass-spring system.

1. Introduction

A recent collapse of a pedestrian walkway bridge in North Carolina, USA (http://www.cnn.com/2000/US/05/21/walkway.collapse) has received a tremendous media's attention emphasising the importance of the health and condition monitoring for such structures. Furthermore, we are on the brink of a major technical upheaval making the development of such a monitoring system feasible.

Rytter (1993) categorised the damage monitoring process into four stages: (1) identification of the damage presence in the structure, (2) localisation of the damage, (3) quantification of the damage severity, (4) prediction of the remaining service life of the structure. Doebling et al. (1998) present a recent thorough review of the vibration-based damage identification methods. While the references cited in this review propose many different methods for identifying and localising damage from vibration response measurements, the majority of the cited references rely on cumbersome finite element modelling process and/or linear modal properties for damage diagnosis.

The authors have been tackling the damage detection problems based exclusively on the statistical analysis of time series. The structural health-monitoring problem is posed in the context of a statistical pattern recognition paradigm. This paradigm can be described as a four-part process: 1.) operational evaluation, 2.) data acquisition & cleansing, 3.) feature extraction & data reduction, and 4.) statistical model development. In particular, this paper focuses on Parts 3 and 4 of the process. More detailed discussion of the statistical pattern recognition paradigm can be found in Farrar et al, 2000. It should be noted that neither any sophisticated finite element models nor the traditional modal parameters are employed in this paradigm because they often require labour intensive tuning and result in erroneous uncertainties caused by user interaction and modelling errors. The approach presented here is solely based on signal analysis of the measured vibration data making this approach very attractive for the development of an automated health monitoring system. This signal-only-based paradigm has been applied to the damage identification problem by the authors (Sohn et al., 2000 and Fugate et al., 2000). In this paper, we are extending this paradigm to the second level damage diagnosis, *damage localisation problems*. The applicability of the proposed approach is investigated using a simple 8 DOF mass-spring system tested in a laboratory environment.

2. Test Structure

An eight degrees-of-freedom system has been designed and constructed to study the effectiveness of the proposed localisation procedure. The system is formed with eight translating masses connected by springs. The

[1] 505-667-6135 (Voice), 505-665-7836 (Fax), sohn@lanl.gov (E-mail).
[2] 505-667-4551 (Voice), 505-665-2137 (Fax), farrar@lanl.gov (E-mail).

system employed in this study is shown in Figure 1. Each mass is a disc of aluminium 25.4 mm thick and 76.2 mm in diameter with a center hole. The hole is lined with a Teflon bushing. There are small steel collars on each end of the discs. The masses all slide on a highly polished steel rod that supports the masses and constrains them to translate along the rod. The masses are fastened together with coil springs epoxied to the collars that are, in turn, bolted to the masses.

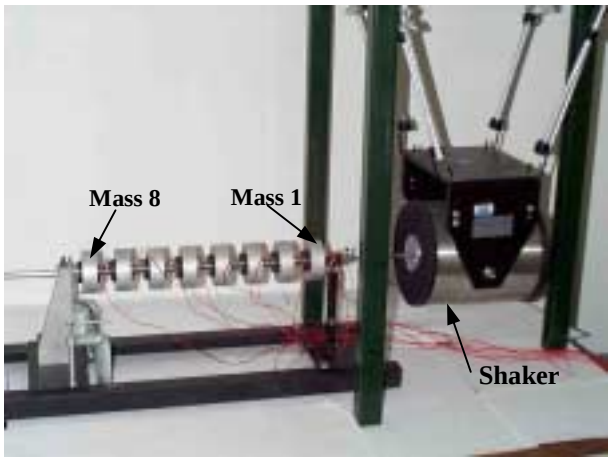

Figure 1: An eight degrees-of-freedom system attached to a shaker with accelerometers mounted on each mass

DOFs, springs and masses are numbered from the right end of the system, where the excitation is applied, to the left end as shown in Figure 1. The nominal value of mass 1 is 559.3 grams. Again, this mass is located at the right end where the shaker is attached. Mass 1 is greater than the others because of the hardware needed to attach the shaker. All the other masses (mass 2 through mass 8) are 419.4 grams. The spring constant for all the springs is 56.7 kN/m (322 lb/in) for the initial condition

Damping in the system is caused primarily by Coulomb friction. Every effort is made to minimise the friction through careful alignment of the masses and springs. A common commercial lubricant is applied between the Teflon bushings and the support rod.

Measurements made during damage identification tests are the excitation force applied to mass 1 and the acceleration response of all masses. Random excitation is accomplished with a 215-N (50 lb) peak force electro-dynamic shaker (Figure 1). The root-mean – square (RMS) amplitude level of the input is varied from 3 volts to 7 volts. All the time history data presented here are recorded with the 3 volt input level unless specified.

The data acquisition equipment used in this study was a Hewlett- Packard 3566A data acquisition system. A laptop computer was used for data storage and as the platform for the software for controlling the data acquisition system. The force transducer used has a nominal sensitivity of 22.48 mv/N (100 mv/lb), and the accelerometers have a nominal sensitivity of 10 mv/g. The detailed specifications for the data acquisition are presented in Table 1.

Table 1: Specifications for data acquisition

Time step	0.001953 sec.
Sampling rate	512 Hz
Time period	8 sec.
Frequency resolution	0.125Hz
Number of data points	4096
Filtering	Uniform window
Nyquist frequency	256Hz

The undamaged configuration of the system is the state for which all springs are identical and have a linear spring constant. Two types of damage, linear or nonlinear damage, are simulated. Either type of damage may be located between any adjacent masses in the system.

Linear damage is defined as a change in the stiffness characteristics of the system such that the system can still be modelled by the standard linear differential equations of motion for a vibrating system after the damage. Linear damage in the model is simulated by replacing an original spring with another linear spring which has a spring constant less than that of the original. The spring constant is gradually reduced to 52.6 kN/m (299 lb/in) (7 % reduction), 49.0 kN/m (278 lb/in) (14% reduction), and 43.0 kN/m (244 lb/in) (24% reduction) for selected spring locations, respectively. The replacement spring is located between any adjacent masses, and thus simulates different locations of damage. The replacement springs have different degrees of stiffness reduction to simulate different levels of damage.

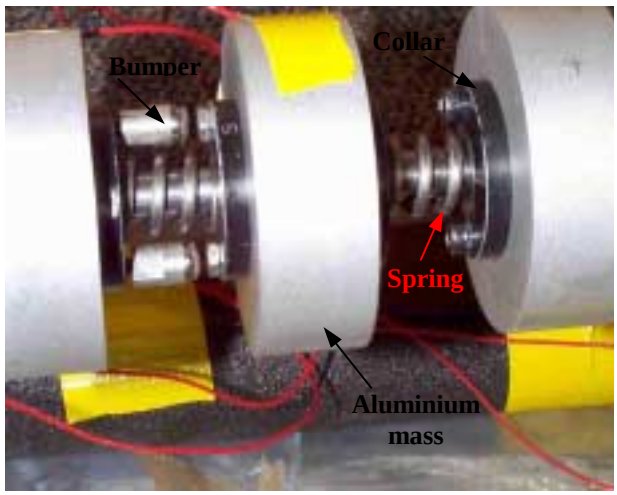

Figure 2: A typical bumper used to simulate nonlinear damage

Nonlinear damage is defined as an occurrence of impact between two adjacent masses. It is simulated by placing a bumper on one mass that limits the amount of motion that mass may move relative to the adjacent mass. Figure 2 shows the hardware used to simulate

nonlinear damage. When the distance between mass and the ends of the rods is equal to the initial clearance, impact occurs. This impact simulates damage caused by spring deterioration to a degree which permits contact between adjacent masses, or in a simplified manner, the impact from the closing of a crack during vibration. The degree of damage is controlled by changing the amount of relative motion permitted before contact, and changing the hardness of the bumpers on the impactors.

3. Analysis Procedure

A linear prediction model combining AR and ARX models is employed in this study to compute our damage-sensitive feature, the residual error.

First, all time signals are normalized prior to fit an AR model such that:

$$\hat{x} = \frac{x - \mu_x}{\sigma_x} \qquad (1)$$

where $\hat{x}$ is the normalized signal, μ_x and σ_x are the mean and standard deviation of *x*, respectively. This normalization procedure is applied for all signals employed in this study. (However, for simplicity, *x* is used to denote $\hat{x}$ hereafter.)

Then, we construct an AR model with *p* auto-regressive terms, AR(*p*), using the time series obtained at the initial condition of the structure, *x(t)*. In this example, AR(30) is constructed and an AR(*p*) model can be written as (Box et al., 1994) :

$$x(t) = \sum_{j=1}^{p} \phi_{xj}\ x(t-j)\ + e_x(t) \qquad (2)$$

Employing a new segment *y(t)* obtained from unknown structural condition of the system, repeat Equation (2). Here the segment $y(t)$ has the same length as segment $x(t)$:

$$y(t) = \sum_{j=1}^{p} \phi_{yj}\ y(t-j)\ + e_y(t) \qquad (3)$$

Next, we assumed that the error between the measurement and the prediction obtained by the AR model ($e_x(t)$ in Equation (2)) is mainly caused by the unknown external input. Based on this assumption, we employ an ARX model (Auto-Regressive model with eXogenous inputs) to reconstruct the input/output relationship between $e_x(t)$ and $x(t)$.

$$x(t) = \sum_{i=1}^{a} \alpha_i\ x(t-i)\ + \sum_{j=0}^{b} \beta_j\ e_x(t-j) + \varepsilon_x(t) \qquad (4)$$

where $\varepsilon_x(t)$ is the residual error after fitting the ARX(*a,b*) model to the $e_x(t)$ and $x(t)$ pair. Our feature for the classification of damage status will later be related to this quantity, $\varepsilon_x(t)$. ARX(25,25) is used in this example. Here, the *a* and *b* values of the ARX model are set rather arbitrarily. However, similar results are obtained for different *a* and *b* values as long as the sum of *a* and *b* is kept smaller than *p* ($a + b \le p$).

Next, we investigate how well the ARX(*a,b*) model estimated in Equation (4) reproduces the input/output relationship of $e_y(t)$ and $y(t)$:

$$\varepsilon_y(t) = y(t)\ - \sum_{i=1}^{a} \alpha_i\ y(t-i)\ - \sum_{j=0}^{b} \beta_j\ e_y(t-j) \qquad (5)$$

where $e_y(t)$ is considered to be an approximation of the system input estimated from Equation (3). Again, note that the α_i and β_j coefficients are associated with $x(t)$ and obtained from Equation (4). Therefore, if the ARX model obtained from the reference signal block $x(t)$ were not a good representative of the newly obtained signal segment $y(t)$ and $e_y(t)$ pair, there would be a significant change in the probability distribution of the residual error, $\varepsilon_y(t)$. Particularly, the standard deviation of the residual error, $\sigma(e_y)$, is expected to increase at most near the actual damage sources providing the localisation information of damage.

4. Analysis Results

For the localisation of nonlinear damage, three different damage scenarios are studied varying the damage locations. For each damage case, five sets of time histories are recorded. Table 2 summarises the damage cases studied in this example.

Table 2: List of studied nonlinear damage scenarios

Damage scenarios	Damage description	Type of excitation	Test #
1	No damage	Random, 3Volts	5
2	Bumper at mass 1	Random, 3Volts	5
3	Bumper at mass 5	Random, 3Volts	5
4	Bumper at mass 7	Random, 3Volts	5

First, the α_i and β_i coefficients in Equation (4) are computed for an individual DOF using one of the five time series obtained under the undamaged state of the structure. Next, the residual error, $e_y(t)$, in Equation (5) is computed for all damage cases.

Table 3 summarises the standard deviation of the residual errors, $\sigma(e_y)$, for each DOF and all damage cases and Table 4 shows the mean $\sigma(e_y)$ values for an individual damage case with respect to DOFs. If a bumper were introduced at mass 1, the largest increase in the residual standard deviation would be expected at the nearest measurement point, DOF 1. As shown in Table 3, no significant increase in $\sigma(e_y)$ was found for DOF 1 when the bumper was introduced at mass 1. Instead, the $\sigma(e_y)$ value in the next adjacent measurement point, DOF 2, was significantly increased

from 0.1229 to 1.0005 on average (see Figure 3(a)). It is speculated that because DOF 1 is rigidly connected to the shaker by a rod, the response at this point is masked by the direct influence of the random input.

When the bumper was placed at mass 5, the average $\sigma(e_y)$ value in DOF 5 increased from 0.1352 to 1.1670 marking the largest increase among all DOFs (see the fourth row of Table 4 and Figure 3(b)). A similar result is observed when the bumper is placed at mass 7 (Figure 3(c)). Here a simple chart of the $\sigma(e_y)$ values with respect to DOFs seems to reveal the approximate location of the nonlinear damage as shown in Table 4. However, in order to establish a rigorous threshold value, test data need to be acquired under different operational conditions, and the probability distribution of $\sigma(\varepsilon_y)$ first needs to be estimated. Because the data sets given to us are limited, the construction of the threshold value based on a rigorous statistical analysis is not achieved in this example.

In reality, the influences of operational and environmental conditions to the residual error need to be addressed. For example, the amplification of the input force can also introduce amplitude-dependent nonlinearity resulting in the increase in $\sigma(e_y)$. Table 5 illustrates that the $\sigma(e_y)$ values gradually increase in accordance with the level of input amplitude.

The authors have been investigating a data normalisation procedure to differentiate the effects of these environmental and/or operation conditions to the residual errors from these of structural characteristics of our interest, damage (Sohn et al, 2001). The application of this data normalisation procedure to this example will be presented in near future.

Table 3: Standard deviation of the residual errors $\sigma(e_y)$ for various damage scenarios

Data set #	No damage	Bumper at m1	Bumper at m5	Bumper at m7
DOF 1				
1	0.0226†	0.1708	0.1229	0.1615
2	0.1547	0.1533	0.1112	0.1580
3	0.1136	0.1756	0.1112	0.1427
4	0.1059	0.1841	0.1527	0.1613
5	0.1153	0.1834	0.1317	0.1767
Mean	**0.1024**	**0.1735**	**0.1259**	**0.1600**
DOF 2				
1	0.0304†	0.9665	0.2196	0.2744
2	0.1919	1.0063	0.2128	0.2600
3	0.1069	1.0217	0.2128	0.2896
4	0.1488	1.0145	0.2543	0.3407
5	0.1366	0.9935	0.2190	0.3030
Mean	**0.1229**	**1.0005**	**0.2237**	**0.2935**
DOF 3				
1	0.0014†	0.4688	0.2323	0.2913
2	0.1947	0.5474	0.2215	0.3288
3	0.1300	0.5464	0.2215	0.2947
4	0.1446	0.5254	0.2413	0.3334
5	0.1590	0.5058	0.2326	0.3001
Mean	**0.1259**	**0.5188**	**0.2298**	**0.3097**
DOF 4				
1	0.0025†	0.2891	0.2893	0.3545
2	0.1802	0.2957	0.2276	0.3672
3	0.1309	0.2826	0.2276	0.3765
4	0.1601	0.3341	0.2825	0.4063
5	0.1476	0.2788	0.2847	0.3721
Mean	**0.1243**	**0.2961**	**0.2623**	**0.3753**
DOF 5				
1	0.0041†	0.3524	1.1248	0.3976
2	0.2036	0.3703	1.1095	0.4185
3	0.1321	0.3771	1.1095	0.3705
4	0.1703	0.3870	1.3184	0.3971
5	0.1659	0.5001	1.1730	0.4248
Mean	**0.1352**	**0.3974**	**1.1670**	**0.4017**
DOF 6				
1	0.0002†	0.2560	0.3600	0.6425
2	0.1515	0.2135	0.3406	0.6342
3	0.1061	0.2003	0.3406	0.6463
4	0.1247	0.2480	0.3505	0.6472
5	0.1233	0.3733	0.2913	0.6376
Mean	**0.1012**	**0.2582**	**0.3366**	**0.6416**
DOF 7				
1	0.0035†	0.2219	0.1941	0.6714
2	0.1854	0.1877	0.1481	0.6870
3	0.1241	0.2307	0.1481	0.6185
4	0.1210	0.2742	0.1984	0.6705
5	0.1633	0.2169	0.1440	0.6799
Mean	**0.1195**	**0.2263**	**0.1666**	**0.6655**
DOF 8				
1	0.0030†	0.1702	0.2111	0.1918
2	0.1480	0.1572	0.1367	0.2151
3	0.1140	0.1726	0.1367	0.2400
4	0.1161	0.1961	0.1457	0.2455
5	0.1296	0.1521	0.1522	0.2271
Mean	**0.1021**	**0.1696**	**0.1565**	**0.2239**

† The standard deviations for these data sets are significantly smaller than the others because they are used for both the estimation of the ARX model and prediction.

5. Conclusion

An attempt is made to locate the damage locations within a mechanical system solely based on the time series analysis of vibration test data. The standard deviation of the residual errors, derived from a combination of AR and ARX models, is used to locate damage. A noticeable increase in this residual standard deviation is observed near the actual damage regions. The presented approach is very attractive for the development of an automated continuous monitoring system because of its simplicity and no interaction with users. Furthermore, because damage diagnosis is conducted independently at an individual sensor level, time synchronisation among the multiple sensors is not necessary. However, it should be pointed out that the procedure developed has only been verified on a limited amount of data. Ideally, it would be necessary to examine many time records corresponding to a wide range of operational and environmental cases as well as different damage scenarios before one could state with

confidence that the proposed method is robust enough to be used in practice.

References

1. Box, G. E., Jenkins, G. M., and Reinsel, G. C., *Time Series Analysis: Forecasting and Control*, Third Edition, Prentice-Hall, Inc., New Jersey, 1994.
2. Doebling, S. W., Farrar, C. R., Prime, M. B., and Shevitz, D. W., "A Review of Damage Identification Methods that Examine Changes in Dynamic Properties," *Shock and Vibration Digest* **30** (2), 1998.
3. Farrar, C. R., Duffey, T. A., Doebling, S. W., Nix, D. A., "A Statistical Pattern Recognition Paradigm for Vibration-Based Structural Health Monitoring," Proceedings of the 2nd International Workshop on Structural Health Monitoring, Stanford, CA, USA, pp. 764-773, September 8-10, 2000.
4. Fugate, M. L. Fugate, Sohn, H. and Farrar, C. R., "Vibration-Based Damage Detection Using Statistical Process Control," *accepted for publication in Mechanical Systems and Signal Processing*, 2000.
5. Rytter, A., 1993. "Vibration Based Inspection of Civil Engineering Structures", Ph. D. Dissertation, Department of building Technology and Structural Engineering, Aalborg University, Denmark.
6. Sohn, H. Farrar, C. R., and Hunter, N. F., "Data Normalization Issue for Vibration-Based Structural Health Monitoring," *accepted for presentation at the 19th International Modal Analysis Conference*, Orlando, FL, USA, February 5-8, 2001.
7. Sohn, H., Czarnecki, J. J., and Farrar, C. R. Farrar, "Structural Health Monitoring using Statistical Process Control and Projection Techniques," *accepted for publication in Journal of Engineering Mechanics, ASCE*, 2000.

Table 4: Mean standard deviation of the residual errors $\sigma(e_y)$ for all DOFs and damage scenarios

Bumper Location	DOF 1	DOF 2	DOF 3	DOF 4	DOF 5	DOF 6	DOF 7	DOF 8
No	0.1024	0.1229	0.1259	0.1243	0.1352	0.1012	0.1195	0.1021
at m1	0.1735	**1.0005**	0.5188	0.2961	0.3974	0.2582	0.2263	0.1696
at m5	0.1259	0.2237	0.2298	0.2623	**1.1670**	0.3366	0.1666	0.1565
at m7	0.1600	0.2935	0.3097	0.3753	0.4017	0.6416	**0.6655**	0.2239

Table 5: The variation of the residual errors $\sigma(e_y)$ for various input levels (obtained from DOF 8)

Data set #	Input Excitation				
	3 Volts	4 Volts	5 Volts	6 Volts	7 Volts
1	0.0120	0.2528	0.3564	0.4645	0.6967
2	0.1700	0.2070	0.4210	0.4299	0.7175
3	0.1379	0.2256	0.2669	0.4515	0.7888
4	0.1410	0.2295	0.2251	0.4256	0.7425
5	0.1456	0.1919	0.3606	0.4645	0.8227
Mean	**0.1213**	**0.2214**	**0.3260**	**0.4472**	**0.7536**

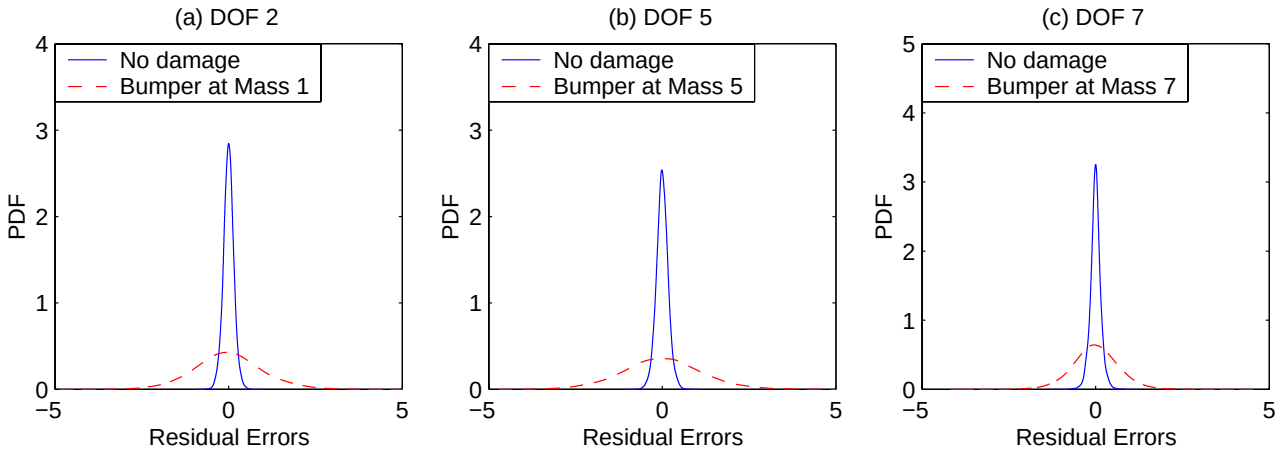

Figure 3: Comparison of the probability density functions for different damage cases